(2)

AEOSR-TR- 92 0779

Annual Technical Report
on

HIGH-POWER MICROWAVE BREAKDOWN OF DIELECTRIC INTERFACES

July 15, 1992

Air Force Office of Scientific Research
Grant No. 91-0260

PULSED POWER LABORATORY
DEPARTMENT OF ELECTRICAL ENGINEERING
TEXAS TECH UNIVERSITY
LUBBOCK, TEXAS 79409-3102

"The views and conclusions contained in this document are those of the authors and should not be interpreted as necessarily representing the official policies or endorsements, either expressed or implied, of the Department of the Air Force of the United States Government."

REPORT DOCUMENTATION PAGE

Form Approved
OMB No. 0704-0188

1. AGENCY USE ONLY (Leave blank)	2. REPORT DATE	3. REPORT TYPE AND DATES COVERED
	15 July 1992	Annual Technical, 15 April 1991-14 April 1992

4. TITLE AND SUBTITLE

HIGH POWER MICROWAVE BREAKDOWN OF DIELECTRIC INTERFACES

5. FUNDING NUMBERS

AFOSR-91-0260

6. AUTHOR(S)

M. Kristiansen, L.L. Hatfield, and Mark Crawford

7. PERFORMING ORGANIZATION NAME(S) AND ADDRESS(ES)

Texas Tech University
Dept. of Electrical Engineering
P.O. Box 43102
Lubbock, TX 79409

8. PERFORMING ORGANIZATION REPORT NUMBER

9. SPONSORING/MONITORING AGENCY NAME(S) AND ADDRESS(ES)

AFOSR/NE
Bldg. 410
Bolling AFB, DC 20332

10. SPONSORING/MONITORING AGENCY REPORT NUMBER

2301 ES

11. SUPPLEMENTARY NOTES

12a. DISTRIBUTION/AVAILABILITY STATEMENT

unlimited

12b. DISTRIBUTION CODE

13. ABSTRACT *(Maximum 200 words)*

The objective of this project is to study the electrical breakdown, due to microwaves, which occurs on the surface of vacuum/atmosphere interfaces. This is an annual technical report for AFOSR Grant No. 91-0260, that began in April, 1991 and concluded one year later. This contract was continuing work started on AFOSR Grant No. 88-0102. The final report for that grant was submitted in November, 1991.

This report will discuss results relating to: placing magnets on the waveguide to prevent the electron beam from hitting the window, frequency measurements of the microwave signal, and the design, construction, and testing of a device for reducing window breakdown.

14. SUBJECT TERMS	15. NUMBER OF PAGES
Microwaves, window-breakdown, surface flashover, radio frequency	12
	16. PRICE CODE

17. SECURITY CLASSIFICATION OF REPORT	18. SECURITY CLASSIFICATION OF THIS PAGE	19. SECURITY CLASSIFICATION OF ABSTRACT	20. LIMITATION OF ABSTRACT
Unclassified	Unclassified	Unclassified	

Summary

The objective of this project is to study the electrical breakdown, due to microwaves, which occurs on the surface of vacuum/atmosphere interfaces. This is an annual technical report for AFOSR Grant No. 91-0260, that began in April, 1991 and concluded one year later. This contract was continuing work started on AFOSR Grant No. 88-0102. The final report for that grant was submitted in November, 1991.

Since November, 1991, the research has been slowed due to several factors. First, since the graduation of a Ph.D. student, there has been only one graduate student working on the project. Also, in an attempt to run the system at consistently higher power than previous work had allowed, several weak points in the system had to be identified and corrected. Finally, a utility outage caused a massive vacuum failure requiring complete disassembly, cleaning and repairing, and reassembly of all systems connected to the vacuum chamber. Due to these problems, several ideas for improving window performance have yet to be implemented.

This report will discuss the results that were obtained. Magnets were placed on the waveguide to determine if the electron beam was hitting the window. Frequency measurements were taken and a new tuning stub was designed, constructed, and mounted to reduce the microwave power density at the window.

Project Overview

The electrical breakdown of a dielectric window in the atmosphere due to a high-power microwave pulse has been investigated. Electrical breakdown of the window creates a plasma, through which the microwaves cannot propagate or are attenuated and/or refracted. Several factors have been studied, including the effects of different window materials, window shapes, window coatings, and ambient gases. Most of that work was completed under the previous contract. Under the present contract, devices at the end of the waveguide designed to mitigate the breakdown were studied. If the breakdown strength can be improved, the microwave power through the window can be increased.

The high-power microwaves are produced by a virtual cathode oscillator (vircator)[1]. An overall schematic drawing of the equipment is shown in Figure 1. An electron beam is injected into a waveguide where the space-charge limit is exceeded, a virtual cathode that oscillates in space and time is formed, and the microwaves are extracted. The experiment consists of a 10 Ω, 12.5 ns one-way transit time, coaxial pulse forming line (PFL) that is charged from a Marx bank and switched into the vacuum diode through a self-breaking spark gap. The Marx tank, PFL, and output switch are all filled with transformer oil. The vacuum diode and the waveguide are evacuated with a diffusion pump and two mechanical roughing pumps. The best vacuum attained to date has been better than 1×10^{-6}. The end of the waveguide where the window is located is contained in an anechoic chamber which provides a reflection-free environment in which to observe the breakdown and measure microwave power.

The diagnostic system is able to directly measure the Marx bank voltage, diode current, diode voltage, microwave power density at a given location in the radiation pattern, and the temporal variations in the light from the breakdown. In addition, two mechanical cameras are placed to capture time-integrated photographs from inside the anechoic chamber. One camera views the window and captures the breakdown image, the other photographs the radiation pattern as detected by an array of fluorescent tubes placed at the end of the anechoic chamber.

In addition to the actual experimental equipment, a great deal of research has been done using the simulation code MAGIC[2]. MAGIC is a two-and-one-half dimensional, fully relativistic, particle-in-cell code. Using various university computing facilities, a number of simulations have been run to investigate the operation of the vircator and waveguide.

Research Results

It was suggested that electrons from the vacuum diode might be impacting on the window. If so, such a phenomenon might influence the breakdown on the surface of the window. Several options were considered to determine if, indeed, the e-beam was hitting the window. The two most obvious solutions were to bend the waveguide so the window would be shaded from the e-beam and to put a transverse magnetic field on the waveguide to bend the electrons into the waveguide wall before they reached the window. Due to the uncertain effect that a bend in the waveguide will have on the mode of microwave propagation, the magnets were chosen as the best solution. Two large permanent magnets were placed on either side of the waveguide. The were oriented so that the e-beam would bend downwards.

When pictures of the microwave induced breakdown on the atmospheric side of the window with and without the magnets were compared, a difference was noticed. Figure 2 is a photo of the breakdown without the magnets on the waveguide. Figure 3 is a photo of the breakdown with the magnets on the waveguide. While there is no basic difference in the breakdown formation, the light that is coming from the window itself is missing in the photo with the magnets. We had previously believed that this light was due to electrical breakdown in the diode which occurred after the microwave generation was complete. That assumption was obviously in error, the light is actually Cerenkov radiation generated when the electron beam runs into the window. Tests run comparing output power with and without the waveguide magnets showed that the magnets did not change the breakdown at the window or power through the window. It is believed that this is because the electrons do not penetrate into the window very deeply and do not have an influence on the atmosphere side of the window.

In order to design a tuning stub for use at the window, it was necessary to measure the microwave frequency obtained at the higher power output. The vircator frequency depends on applied voltage. The frequency of the microwaves had been measured before, but that was taken at lower operating powers. The frequency is measured by taking the output of the microwave B-dot antenna and measuring it directly. Normally the B-dot antenna is connected to a diode detector which gives a power envelope output. The frequency of the microwave is at least 2 GHz which is twice the bandwidth of our fastest oscilloscope. The oscilloscope is analog however, and the high frequency signals are attenuated but the frequency information is not lost. By setting the horizontal sweep rate to 2 ns/div, the microwave signal is quite visible. At this time base setting the screen is

only 20 ns wide and the microwave pulse is much longer than that. In order to capture the entire microwave signal, the machine was fired several times. On each shot the time base was delayed by 15 ns resulting in a series of microwave signal waveforms each showing a different time during the pulse but with a 5 ns overlap with the waveforms before and after it. It was a simple matter to concatenate these individual waveforms into one large data file. By taking the Fast Fourier Transform (FFT) of this large data file, the overall microwave frequency could be determined. The microwave signal in time and frequency is shown in Figure 4. In addition, the data file could be broken into sections of a given time slice and those smaller sections could be FFTed to show an approximation of the temporal development of the microwave frequency. These waveforms are shown in Figure 5.

The geometry which required the frequency information is what we call a "tuning stub." The tuning stub is simply an extension of the waveguide beyond the window. By having the waveguide continue beyond the window, we can take advantage of the wave reflection that occurs at the discontinuity between the end of the waveguide and free space. The length of the waveguide stub is tuned so that maximum destructive interference in the axial electric field occurs at the atmospheric surface of the window. It has been our experience that the axial electric field on the surface of the window is responsible for the initiation of window breakdown. By minimizing this effect, more microwave power ought to propagate through the window without breakdown.

A first approximation of the length of the stub would be $\lambda_g/2$, half of a waveguide wavelength. The fact that this stub occurs so close to the perturbation caused by the window requires that a closer study be done to calculate the ideal stub length. The MAGIC code was used to simulate the electrodynamic system here. By simulating the waveguide and window flange with and without the stub installed, a relative measure of performance between the two can be seen. For each system, an electromagnetic wave is launched down the waveguide which will accurately simulate the microwave frequency and mode in the experiment. Figure 6 shows an output from the simulation for the window with no stub. The top plot is contour plot showing lines of equal axial electric field versus position. The time has been selected to produce a maximum for the axial electric field in the center of the surface of the window. The bottom plot is a plot of the axial electric field in the center of the surface of the window versus time. By carefully evaluating these plots, the axial electric field strength can be determined to be 2.322 MV/m at the center of the surface of the window. While this number has no meaning by itself, when compared to other simulations using the same excitation fields, a relative measure may be deduced. Figure 7 shows the same two plots for the stub of length $\lambda_g/2$. These plots show that the axial electric field strength in the center of the

window is 1.563 MV/m, an improvement of over 35%. By varying the length of the stub, the best length for minimizing the axial electric field can be found. The following is a table showing the results of the simulations.

Length of stub (% of λ_g)	Axial electric field strength	% improvement over no stub
No Stub	2.322 MV/m	--
55.5	1.702 MV/m	26.7%
50.9	1.563 MV/m	32.7%
46.6	1.451 MV/m	37.5%
42.5	1.359 MV/m	41.4%
38.8	1.359 MV/m	41.4%

From the table it can be seen that a minimum should occur between 38.8% and 42.5% of λ_g. By setting the length of the stub to 0.4 λ_g, the maximum amount of destructive interference should occur in the axial electric field at the center of the atmospheric surface side of the window.

The tuning stub was designed so that later, if needed, more attachments could be added onto the end of the stub. A photograph of the stub and window installed on the waveguide is shown in Figure 8. When the experiment was fired, the results were somewhat surprising. A photograph of the window breakdown with the stub installed is shown in Figure 9. When compared to the breakdown without the stub, as shown in Figure 3, the breakdown appears to be longer and thinner when the stub is attached. It is believed that this is due to an increasing axial electric field as one moves from the window to the end of the stub. This field gradient could cause the breakdown plasma to be elongated, even though the axial electric field at the window surface is smaller.

Direct comparisons of power through the window have, to this point, been difficult to obtain. This is because the radiation pattern is changed significantly when the tuning stub is installed. Simulations designed to give a comparison factor have been unsuccessful because of numerical problems involved in making a boundary that does not cause some sort of wave reflection.

It was shortly after these tuning stub experiments began that a failure of the building compressed air supply caused a catastrophic fault in the vacuum system. The inside of the vacuum system was completely coated with a layer of roughing pump oil. The diffusion pump cooked the roughing pump oil into tar and the diffusion pump oil into

glass. After a lengthy disassembly and cleanup of all of the contaminated surfaces, the system has been reassembled and is presently holding a vacuum of 5×10^{-6} Torr.

Future work is planned to finish the tuning stub tests, try one more window shape, and a thin carbon coating on the surface of the window. The window shape is a thin inverted cone. It was determined under the last contract that such a configuration would result in lower axial electric fields on the window surface. The thin carbon coating will hopefully lower the secondary electron emission coefficient of the window surface.

Publications

In the past year one paper was written for publication about several aspects of the research:

M. Crawford, S. Calico, M. Kristiansen, L. Hatfield, "Computer-Assisted Diagnostics on a High-Power Microwave System" presented in poster form and to be published in the proceedings of the XXth International Conference on High-Power Particle Beams in Washington, D.C., June 1992.

Personnel

Principal investigators: Dr. M. Kristiansen, C.B. Thorton/P.W. Horn Professor of Electrical Engineering and Physics
Dr. L.L Hatfield, Professor of Physics

Graduate Students: Mark Crawford earned his M.S.E.E. in August, 1991 and is continuing his research on the experiment for his Ph.D. dissertation.

---

1 V. Grannatstien and I. Alexoff, High Power Microwave Sources Artech House, Boston, 1987.

2 Bruce Goplen, Larry Ludeking, Gary Warren, and Richard Worl, " Magic User's Manual," Mission Research Corporation Technical Report, MRC/WDC-R-246, October 1990

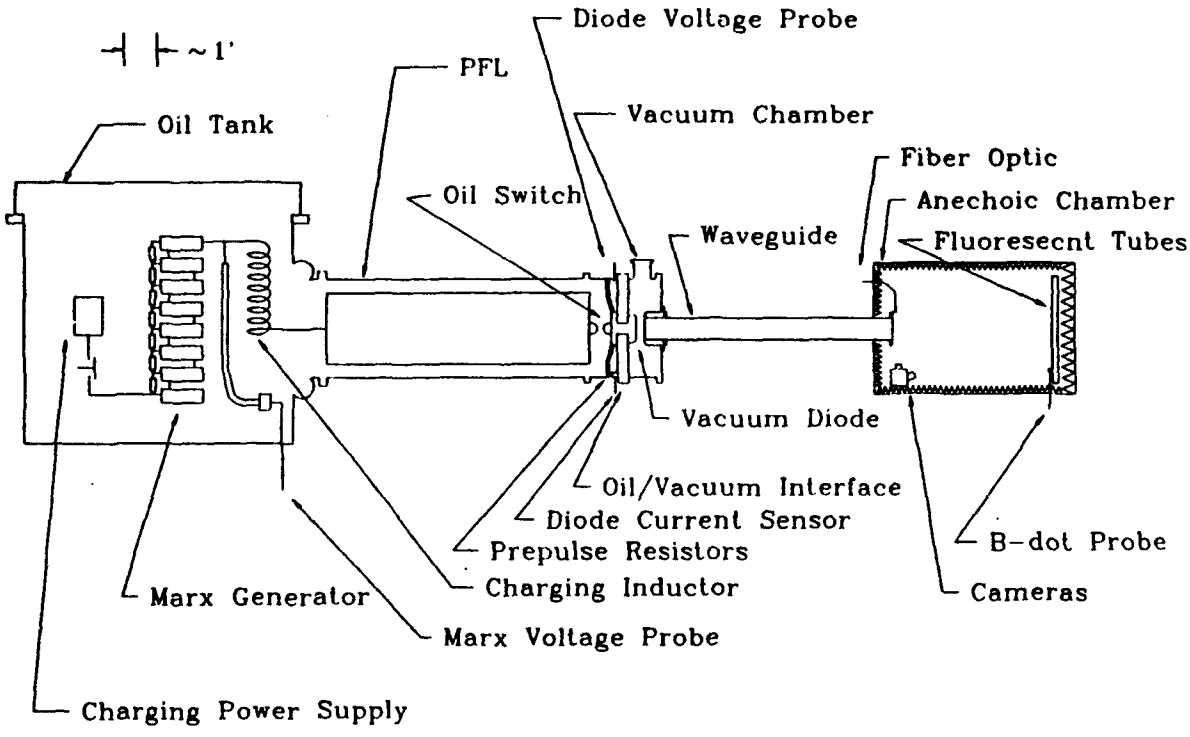

Figure 1. Overall schematic drawing of the equipment.

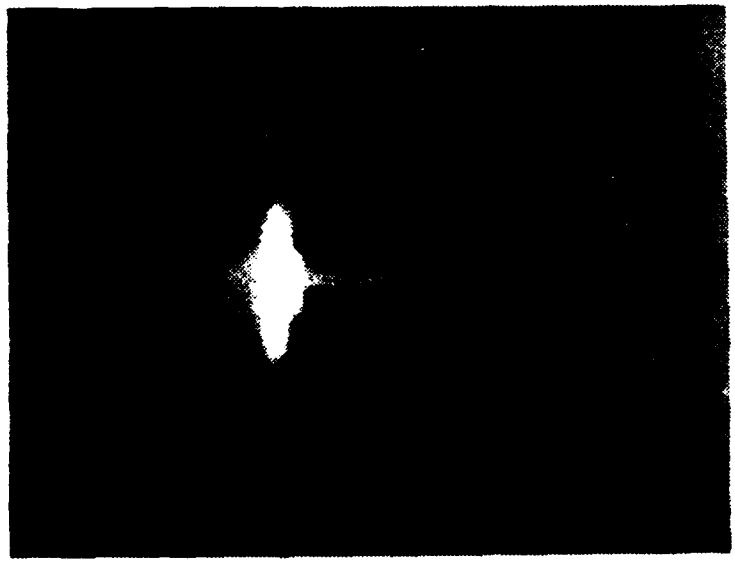

Figure 2. Photograph of the window breakdown without magnets installed on the waveguide.

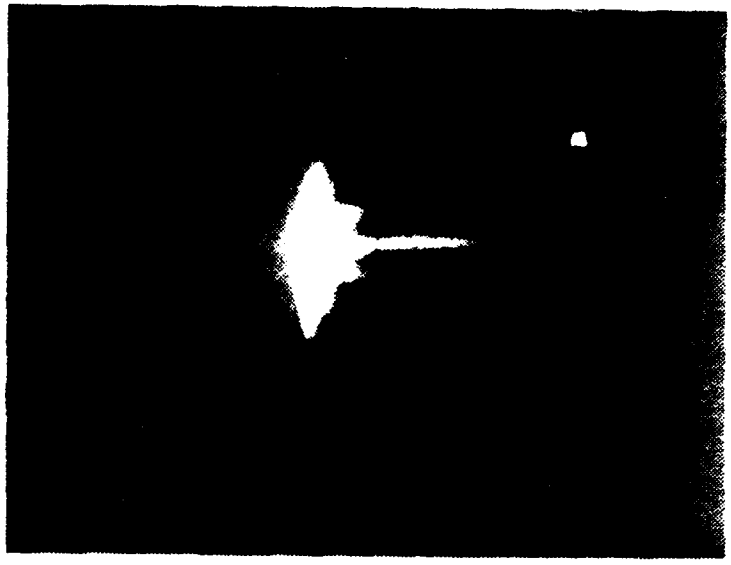

Figure 3. Photograph of the window breakdown with magnets installed on the waveguide

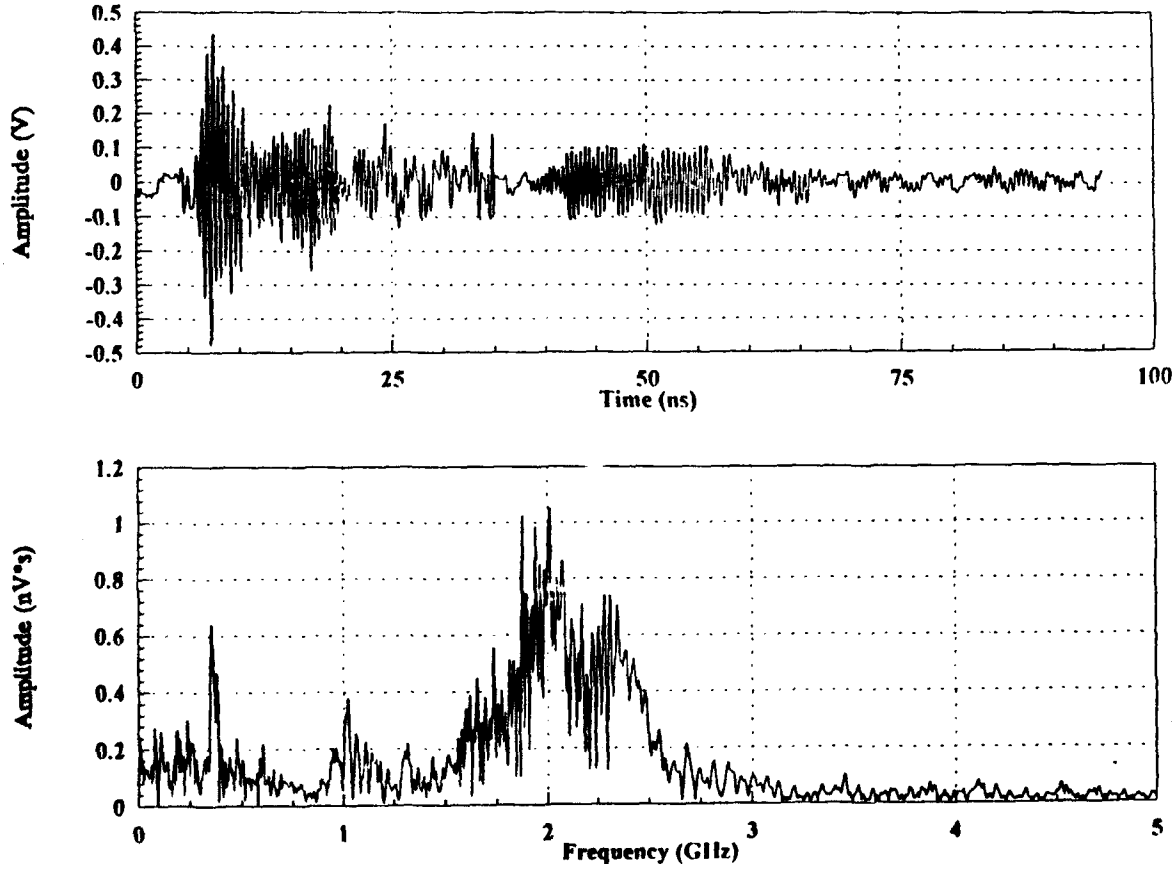

Figure 4. Microwave signal in time and frequency.

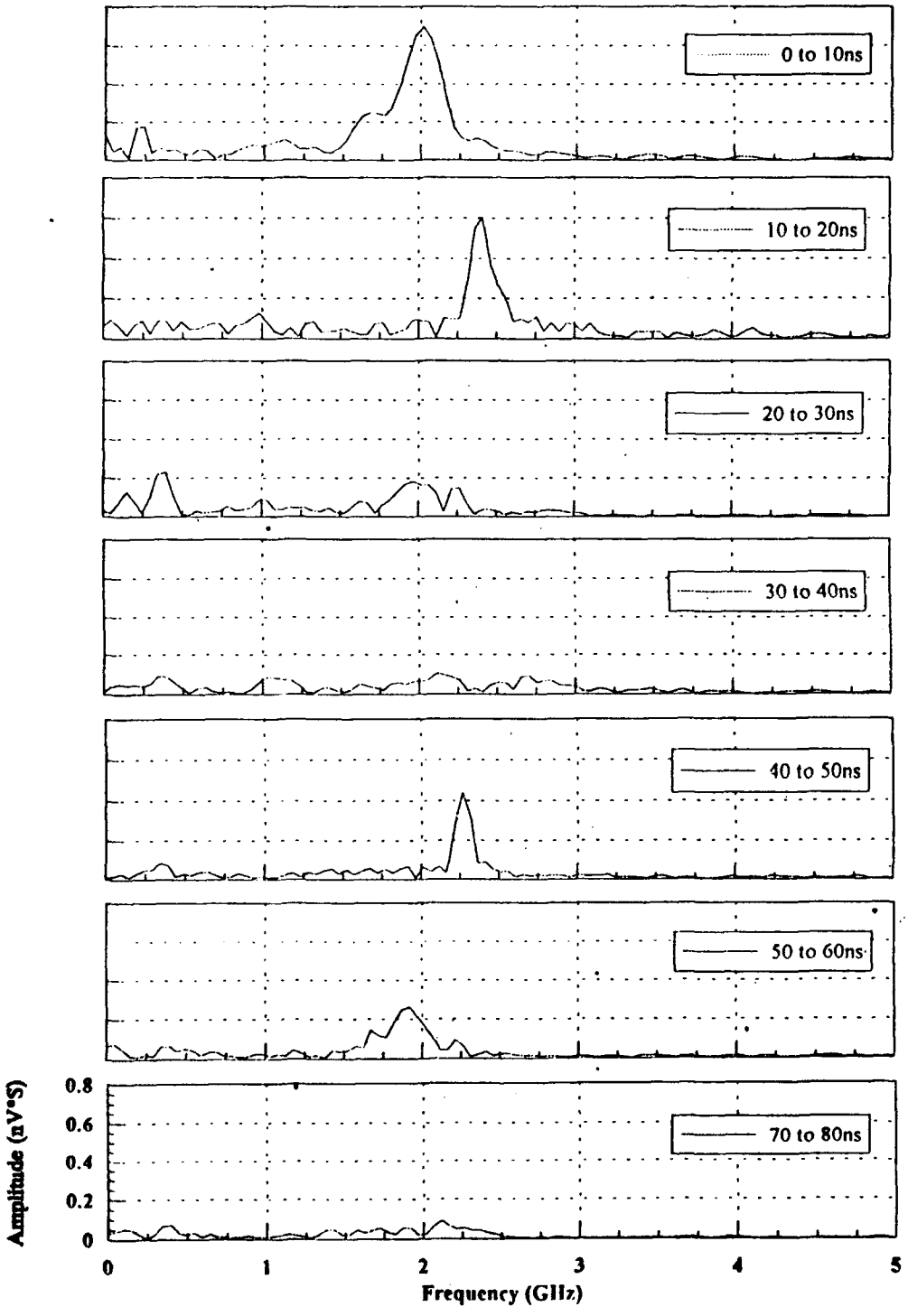

Figure 5. Microwave signal in frequency for various time slices

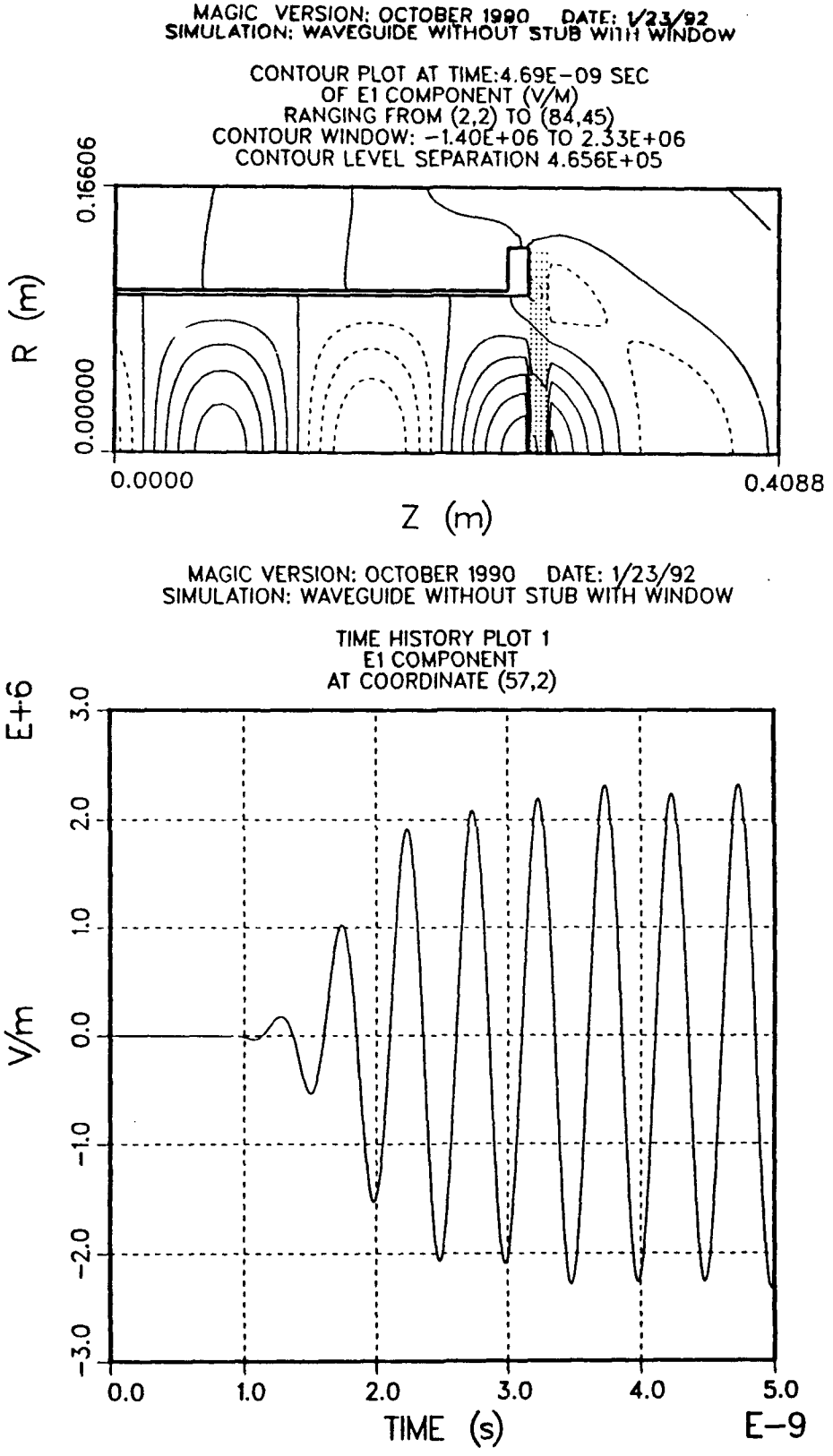

Figure 6. Simulation output for waveguide window with no tuning stub.

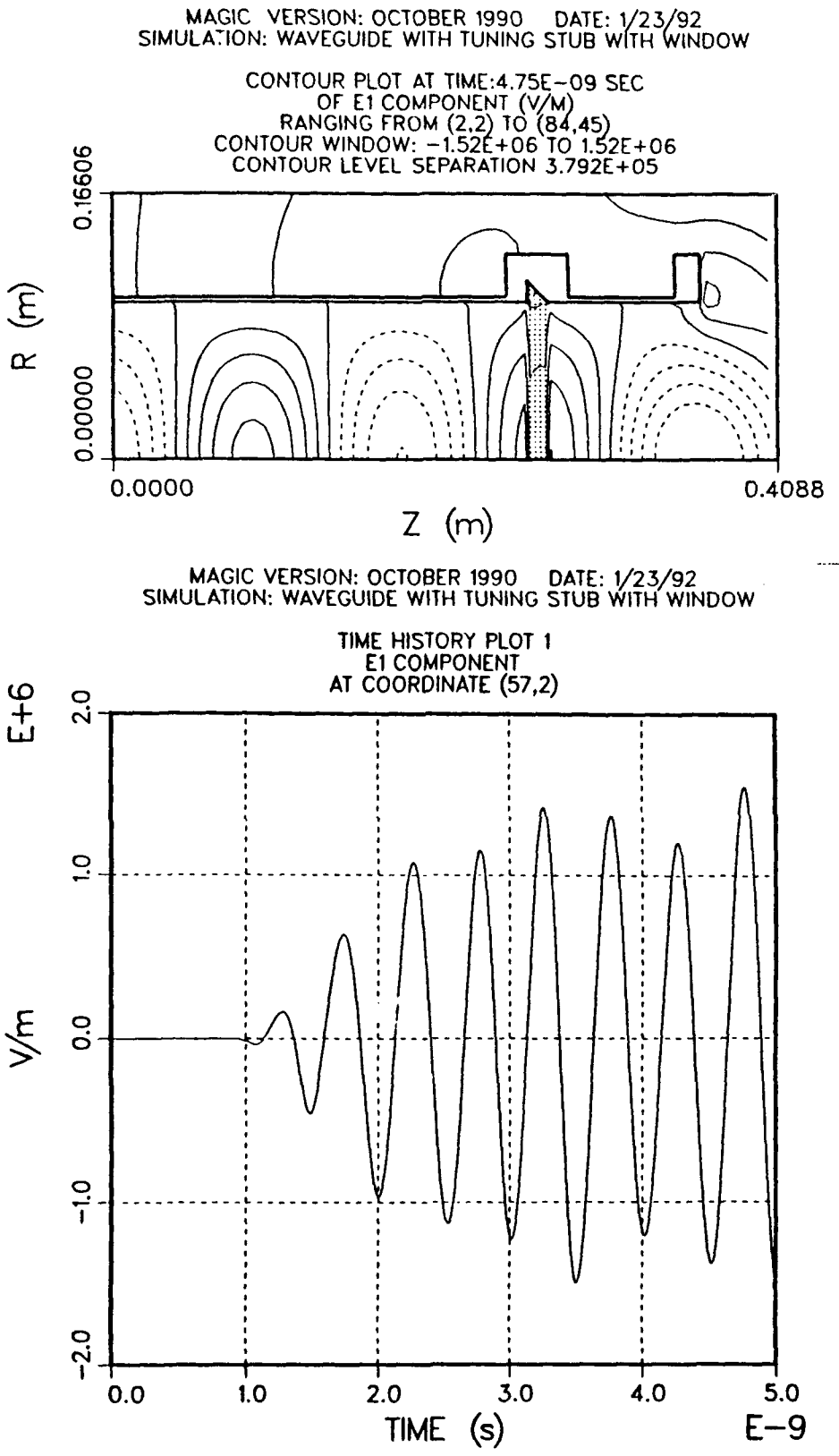

Figure 7. Simulation output for waveguide window with tuning stub of length $\lambda_g/2$.

Figure 8. Photograph of waveguide end with tuning stub installed.

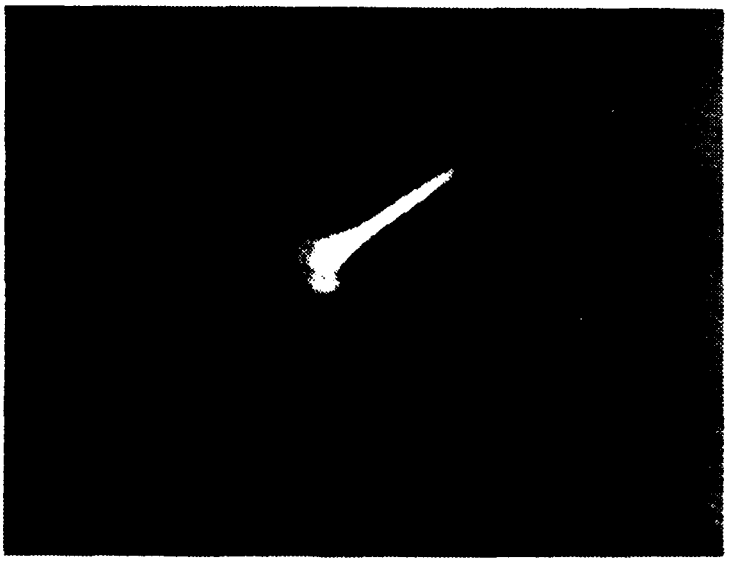

Figure 9. Photograph of window breakdown with tuning stub installed.